

# Identifying evolutionary divergence in gene expression across species and organs: a case-study using Hawaiian *Drosophila*

Samuel H. Church<sup>1,2,\*</sup>      Catriona Munro<sup>3</sup>      Casey W. Dunn<sup>2</sup>  
Cassandra G. Extavour<sup>1,4,5</sup>

<sup>1</sup> Department of Organismic and Evolutionary Biology, Harvard University, Cambridge, MA 02138, USA

<sup>2</sup> Current address: Department of Ecology and Evolutionary Biology, Yale University, New Haven, CT 06520, USA

<sup>3</sup> Collège de France, PSL Research University, CNRS, Inserm, Center for Interdisciplinary Research in Biology, 75005 Paris, France

<sup>4</sup> Department of Molecular and Cellular Biology, Harvard University, Cambridge, MA 02138, USA

<sup>5</sup> Howard Hughes Medical Institute, Chevy Chase, MD 20815

\* corresponding author: [samuelhchurch@gmail.com](mailto:samuelhchurch@gmail.com)

## 1 Abstract

With detailed data on gene expression accessible from an increasingly broad array of species, we can test the extent to which our developmental genetic knowledge from model organisms predicts expression patterns and variation across species. But to know when differences in gene expression across species are significant, we first need to know how much evolutionary variation in gene expression we expect to observe. Here we provide an answer by analyzing RNAseq data across twelve species of Hawaiian *Drosophilidae* flies, focusing on gene expression differences between the ovary and other tissues. We show that over evolutionary time, there exists a cohort of ovary specific genes that is stable and that largely corresponds to described expression patterns from laboratory model *Drosophila* species. However, our results provide a demonstration of the prediction that, as phylogenetic distance increases, variation between species overwhelms variation between tissue types. Using ancestral state reconstruction of expression, we describe the distribution of evolutionary changes in tissue-biased expression, and use this to identify gains and losses of ovary expression across these twelve species. We then use this distribution to calculate the evolutionary correlation in expression changes between genes, and demonstrate that genes with known interactions in *D. melanogaster* are significantly more correlated in their evolution than genes with no or unknown interactions. Finally, we use this correlation matrix to infer new networks of genes that share evolutionary trajectories, and we present these results as a dataset of new testable hypotheses about genetic roles and interactions in the *Drosophila* ovary.

## 2 Introduction

Data on when and where genes are expressed are now fundamental to the study of development and disease<sup>1</sup>. With continually advancing RNA sequencing technologies, these data have been collected using RNA sequencing from a wide variety of cells, treatments and species<sup>2,3</sup>. Statistical analysis of gene expression across these differentials generates insights into how gene expression is connected to phenotypic differences in morphology and behavior<sup>4</sup>. However, when comparing gene expression across species, most studies have been restricted to pairwise comparisons, often between one model laboratory species and one other species of interest<sup>5</sup>. One challenge with such pairwise comparisons is that they lack robust information about how much evolutionary variation in expression we expect to observe, making it difficult to evaluate the significance of any inter-specific difference in variation<sup>5,6</sup>. Instead, we need phylogenetic comparisons of expression that take into account the shared history between species<sup>7,8</sup>, and that describe significant changes in expression in relation to other phenotypic traits of interest.<sup>9</sup> In this study we perform a phylogenetic comparison of gene expression across the organs of twelve species of Hawaiian Drosophilidae flies with highly divergent ovary and egg morphologies. From our results we identify individual genes that have undergone significant evolutionary shifts in organ-specific expression, and describe global patterns in transcriptome variation across species that can serve as a benchmark for future interspecific comparisons of gene expression.

Phylogenetic comparisons of developmental traits are particularly valuable for building context around comparisons between well-studied model organisms and their non-model relatives<sup>10</sup>. Much more has been learned about the genetics and development of laboratory model species like *D. melanogaster* than may ever be possible for the vast majority of life<sup>11</sup>. But the usefulness of model species to understand general principles depends in part on the extent to which biology in these species reflects the biology of other taxa, rather than species-specific phenomena<sup>12</sup>. In the case of gene expression, there has been substantial debate about the degree to which patterns observed in model organisms may be representative across species<sup>13–16</sup>. Where several studies showed that the expression profiles of organs within a species are more different the profiles of homologous organs across species<sup>17–20</sup>, other work has questioned this finding<sup>13,14</sup>. More recently, Breschi and colleagues (2016)<sup>21</sup> demonstrated that, consistent with an evolutionary model of trait evolution, species-level variation in gene expression increases with the time since divergence from the most recent common ancestor. In addition, previous work by authors on this manuscript<sup>8</sup> showed that, while expression patterns across tissues tend to be consistent between species, lineage-specific shifts in expression enrichment can be identified by applying phylogenetic comparative methods. With the exception of the work by Munro and colleagues (2021)<sup>8</sup>, these studies have been, to our knowledge, performed almost exclusively in vertebrate species<sup>17,18,20</sup>, and for the most part placental mammals<sup>13,14,16</sup>, meaning that far less is known about organ and species-level expression differences when comparing across the tree of life.

The detailed atlases of expression data across organs<sup>22</sup> and developmental timepoints<sup>23</sup> is one of the strengths of model systems like *D. melanogaster*. These public resources make it possible to explore global patterns of expression to gain insight into potential gene regulation, interaction, and function<sup>23–25</sup>. As atlases such as these have become increasingly detailed and available from more taxa, a new goal has been to compare these expression profiles across species<sup>7,26,27</sup>. One objective of these cross-species comparisons is to shed light on potential regulatory associations between genes<sup>7,9</sup>. This is especially advantageous for complex processes such as ovarian function for which we have a fragmented understanding of gene regulation despite genetic and transcriptome studies within single model organisms. Another objective of phylogenetic comparisons of expression atlases is to estimate the evolutionary distance between species at which we might expect a given gene to demonstrate a divergent pattern of expression<sup>6</sup>. If this distance is relatively small, then we predict atlases to contain large amounts of species-specific patterns. Alternatively, if as described above, variation across tissues outweighs variation across the species being compared, we predict atlases to contain large cohorts of tissue-specific genes that have been evolutionarily conserved. In this study we test for the existence of a core suite of ovary-specific genes across species of Hawaiian Drosophilidae and describe its size and composition in relation to the described atlas of expression in *D. melanogaster*.

The *Drosophila* ovary has several features<sup>28</sup> that make it a compelling organ in which to test hypotheses about expression evolution. Analyses of the FlyAtlas2 dataset<sup>29</sup> show that in *D. melanogaster*, more genes demonstrate highest expression enrichment in the ovary than any other adult organ (Fig. S1). Additionally,

81 all described signaling pathways are known to have a role in regulating ovarian development<sup>30</sup>. The ovary  
82 performs several critical functions, including maintaining the germ line and manufacturing specialized egg  
83 cells, yolk, and egg-shell materials<sup>31</sup>. Genetic screens<sup>30,32</sup> and experimental manipulation in *D. melanogaster*  
84 have revealed functions of many genes involved in these processes, including yolk-protein genes required  
85 for oogenesis<sup>33</sup> and embryonic patterning genes with localized mRNA like *nanos*<sup>34</sup> and *swallow*<sup>35</sup>. Here  
86 we compare whole-ovary RNA profiles to assess the extent to which these genes and others demonstrate  
87 consistent patterns of ovary-enrichment over evolutionary timescales in a clade with highly divergent ovary  
88 and egg morphologies.

89 The Hawaiian Drosophilidae clade contains an estimated 1,000 extant species<sup>36</sup> that diverged from a common  
90 ancestor with *D. melanogaster* between 25 and 40 million years ago<sup>37</sup>. Extant species have been studied  
91 in particular for the variation in ovary and egg morphology<sup>38,39</sup>. Species of Hawaiian Drosophilidae show  
92 the largest range within the family of egg size, shape, and the number of egg-producing units in the ovary,  
93 known as ovarioles<sup>40-42</sup>. Previous studies by our research group and others have shown that these traits are  
94 likely associated with evolutionary changes in the egg-laying substrate (e.g. rotting bark, flowers, leaves)<sup>38,40</sup>.  
95 Furthermore, our previous work demonstrated that at least one developmental process, governing how the  
96 number of ovarioles is specified in the adult *D. melanogaster* ovary, is conserved in Hawaiian *Drosophila*<sup>40</sup>.  
97 The diversity of Hawaiian species and their relationship to model species make them a strong candidate  
98 model clade for evo-devo research<sup>36,43</sup>. However, their relatively long generation times and species-specific  
99 breeding requirements make laboratory culture more challenging than classic *Drosophila* models<sup>36</sup>. In this  
100 study we leverage technologies that can be deployed on wild-caught individuals to gather rich developmental  
101 data to compare across species.

102 We compared the expression profiles of twelve species of wild-caught Hawaiian Drosophilidae species across  
103 three tissues: the adult ovary, head, and the remaining carcass (Fig. 1). First, we characterized the  
104 differentially expressed genes in the ovary of each species individually. By comparing these to each other,  
105 and to records of ovary-enriched genes from *D. melanogaster*, we identified a core suite of ovary genes shared  
106 across species. We then repeated this analysis for head-enriched genes, and compared the results across  
107 these parallel analyses to test the extent to which global patterns of expression difference are influenced  
108 by the identity of the tissues in question. We applied linear modeling to this dataset to test the overall  
109 contribution of species- and tissue-level differences to expression variation across genes, and describe the  
110 circumstances under which one is likely to dominate over the other. Finally, we used a phylogenetic analysis  
111 of expression changes over evolutionary time to identify genes likely to have gained and lost tissue-enriched  
112 expression. This evolutionary screen of expression changes allowed us to identify networks of genes that  
113 demonstrate correlated changes in expression evolution. We provide these networks as a searchable dataset  
114 of novel, testable hypotheses for gene regulation with respect to ovarian function. The results of this study  
115 demonstrate both the power of Hawaiian *Drosophila* as a model clade for evo-devo, and the potential of using  
116 phylogenetic methods to identify evolutionary variation in gene expression underlying phenotypic differences.

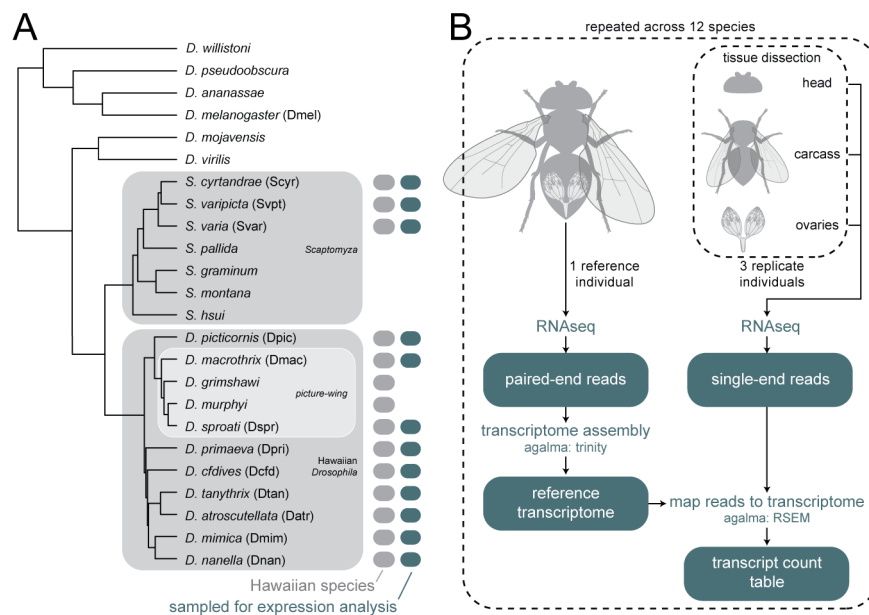


Figure 1: **Phylogeny of species and RNA sampling strategy.** A, Twelve species of Hawaiian Drosophilidae flies were collected in the wild and processed for RNA sequencing. The twelve reference transcriptomes assembled from these species were combined with twelve published genomes to generate the phylogeny shown here (originally published in Church and Extavour, 2021<sup>44</sup>). Three clades within the group are highlighted: the genus *Scaptomyza*, nested within the paraphyletic genus *Drosophila*; the Hawaiian *Drosophila*, which, along with *Scaptomyza*, make up the Hawaiian Drosophilidae; and the well-known *picture-wing* clade. Adjacent to tip labels are four letter species codes used throughout the manuscript. B, The experimental design used to generate the data in this manuscript. When sufficient specimens were available per species, one whole individual was used as a reference and three whole individuals were dissected into three separate tissues: the head, ovaries, and all remaining material (carcass). Reference individuals were sequenced to generate paired-end RNA reads and dissected tissues were sequenced to generate single-end RNA reads. Tissue libraries were then mapped to the assembled reference to quantify transcript expression. Teal boxes indicate data files. Dashed-line boxes indicate a repeated step.

### 3 Results

#### 3.1 Differential gene expression reveals a cohort of consistently ovary-specific genes

We observed several patterns in tissue-specific gene expression that are consistent across all twelve species. First, in all species the main axis of variation separated ovary RNA libraries from head and carcass (Fig. S4). In all species this axis accounted for at least 50% of variation, and in several species greater than 70% of variation. To test for possible variation due to different runs on the sequencer, we resequenced several libraries and compared them using principle component analysis. We found variation between sequencing runs to be negligible compared to variation across tissues and individuals (Fig. S7). Second, in all species we observed that there was a larger amount of significantly downregulated transcripts than upregulated in the ovary relative to the carcass (Fig. 2A-B, S5). Across species, we observed an average of 27.7% to be significantly downregulated and 15.5% of transcripts to be significantly upregulated. In contrast, when comparing the head to the carcass, we observed an average of 10% of transcripts to be significantly upregulated and 10.5% to be significantly downregulated (Fig. S6). Therefore the ovary shows a larger number of both upregulated and downregulated genes relative to the carcass than the head, indicating the ovary has a particularly distinct

132 expression profile. These differences may also reflect variation in the complexity and diversity of functions  
133 of the tissues being compared.

134 We used the results of our differential gene expression analysis within species to test for the existence of a  
135 suite of genes that show consistent ovary-specific expression across species. We found a cohort of 131 genes,  
136 grouped according to BLAST sequence similarity to *D. melanogaster*, for which at least one transcript was  
137 significantly upregulated in the ovaries of more than ten species (Fig. 2C). Transcripts matching these genes  
138 made up on average 24.6% of the significantly ovary-upregulated transcripts across species, indicating that a  
139 substantial portion of ovary-specific genes have conserved expression patterns over evolutionary time (17.7%,  
140 excluding the species *S. varia* that had the most distinct expression profile of all species).

141 We then tested the extent to which these core ovary genes correspond to observations in well-studied labo-  
142 ratory *Drosophila* models. To accomplish this, we compared expression across Hawaiian species to reported  
143 tissue-specific expression levels from *D. melanogaster*<sup>29</sup>. We found that Hawaiian core ovary-specific genes  
144 show nearly universal enrichment in the ovary of *D. melanogaster* as well, as reported in the FlyAtlas2  
145 dataset<sup>29</sup> (Fig. 2D). We likewise observed that genes reported in *D. melanogaster* to have highest enrich-  
146 ment in the ovary largely correspond to genes that are significantly upregulated in the ovaries of Hawaiian  
147 species (Fig. S8).

148 The 131 core ovary genes include several well-known members involved in oogenesis and germline stem cell  
149 renewal such as *nanos*<sup>34</sup>, *swallow*<sup>35</sup>, and *oskar*<sup>45</sup> (Fig. 2E). We found only two genes that were identified as  
150 Hawaiian core ovary genes that are not reported in the FlyAtlas2 dataset<sup>29</sup> to be enriched in the ovary of *D.*  
151 *melanogaster*: the SET domain binding factor *sbf*, and *Rfx*, which are reported to be enriched in the heart,  
152 brain, and other non-reproductive tissues<sup>29</sup>.

153 We used the same approach to identify a core suite of 52 head-specific genes (Fig. S9). There was no  
154 overlap between the sets of core head genes and core ovary genes. To test whether the correspondence  
155 between expression observations in Hawaiian flies and *D. melanogaster* might be due to factors beyond  
156 tissue identity, we compared head expression values to ovary enrichment data from *D. melanogaster*, as we  
157 had done for ovary expression values above. We did not observe a correspondence in either direction between  
158 expression in the head of Hawaiian species and enrichment in the ovary of *D. melanogaster* (Fig. S10A).  
159 In contrast, we did find a correspondence between head-specific expression and genes enriched in the *D.*  
160 *melanogaster* brain, eye, and head (Fig. S10B). Core head genes include *Rhodopsin* photoreceptor genes and  
161 genes such as *hikaru genki* with involvement in synaptic centers<sup>46</sup>.

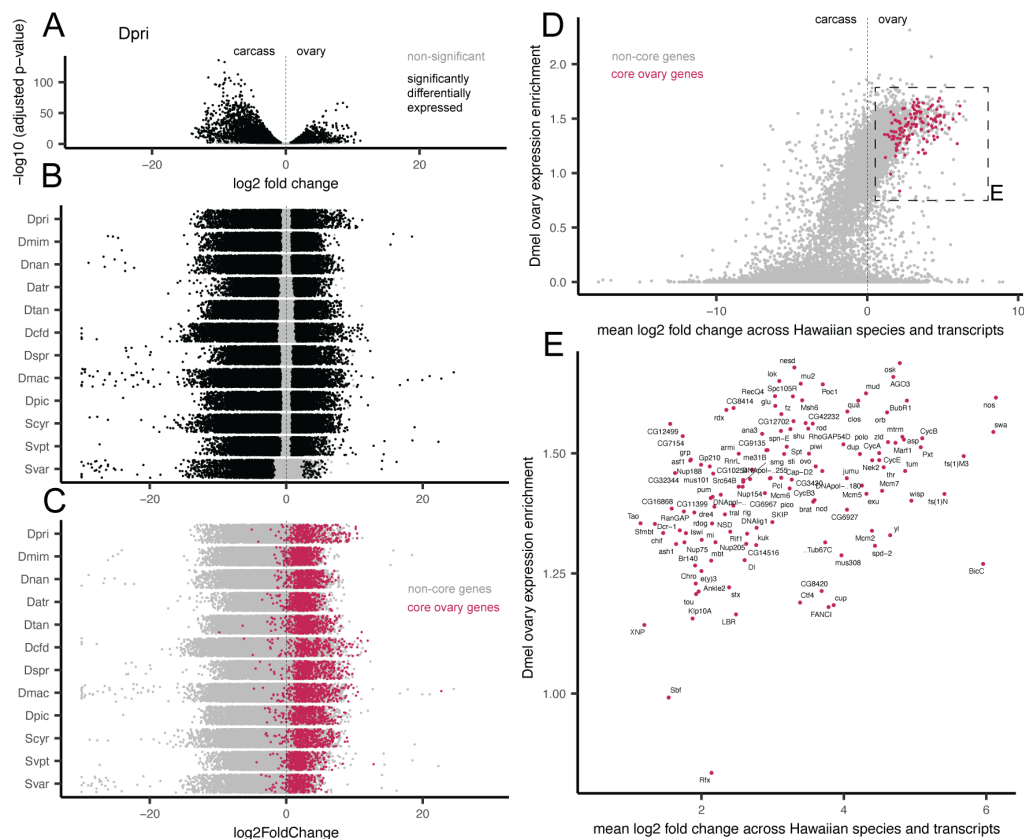


Figure 2: **Identifying a cohort of ovary-specific genes across drosophilid species.** A, Volcano plot for one example species, *D. primaeva* (Dpri), showing the results of a differential gene expression analysis comparing the ovary to the carcass. The x-axis shows the log<sub>2</sub> fold change of expression across transcripts, and the y-axis shows the adjusted p-value, log<sub>10</sub> transformed. Points that are significantly differentially expressed are shown in black. B, Jitter plots showing the results of the same analysis across the twelve species studied here. The x-axis shows the log<sub>2</sub> fold change of expression across transcripts, and points are arranged with random jitter within species on the y-axis. C, The same jitter plots as in B, now colored according to whether or not transcripts belong to a cohort of core ovary genes. These are defined as genes, grouped by BLAST similarity to *D. melanogaster* transcripts, for which at least one transcript is upregulated in the ovary of ten or more of the twelve species. D, A comparison of mean expression change across Hawaiian species to reported ovary-enrichment values from *D. melanogaster*, as reported in FlyAtlas2<sup>29</sup>. Core ovary genes are marked in magenta. E, The boxed region shown in D, magnified and now showing only core ovary genes, annotated with the gene symbol from *D. melanogaster*.

### 3.2 Modeling reveals the phylogenetic decay of expression similarity between tissues

Many studies have investigated the question of whether we expect expression to be more similar across the same organ in different species, or across different organs within the same species<sup>13–20</sup>. Recent studies have suggested that the answer to this question will depend on the phylogenetic distance separating the species being compared<sup>21</sup>. Here we used a modeling approach to investigate this question with respect to the ovaries of Hawaiian drosophilids.

First, we determined an appropriate unit of comparison across species, based on an assessment of homologous features between reference transcriptomes. The agalma pipeline provides a method for determining

171 homologous and orthologous sequences using an all-by-all BLAST approach to determine clusters of recipro-  
172 cally similar sequences (homology groups). These can then be divided into orthology groups by estimating  
173 gene trees and identifying maximally inclusive subtrees with no more than one sequence per taxon<sup>47</sup>. We  
174 compared the representation of species across homology and orthology groups, and observed that while the  
175 representation of homology groups increases with the number of species compared, representation of or-  
176 thology groups decreases (Fig. S11). This is a known obstacle in comparative transcriptomics, attributed  
177 to many transcripts being artifactually fragmented during reference transcriptome assembly<sup>48</sup>. To reduce  
178 the impact of this on our downstream analyses, we averaged TPM values across all transcripts within a  
179 homology group for each sequenced RNA library. Principle component analysis of this average expression  
180 dataset showed that the first principle component divides ovary libraries from the rest, while the second com-  
181 ponent separates samples along an axis that largely corresponds to phylogenetic distance between species  
182 (Fig. S12). While this averaging approach reduces noise due to variable mapping affinities of fragments of  
183 the same transcript, it comes at the cost of averaging over potential variation between genuine transcripts  
184 that fall into the same homology group. Future analyses using improved assemblies for transcriptomes or  
185 genomes will likely be able to avoid this trade off and compare transcript counts directly.

186 With average expression counts for homologous transcripts across species, we tested the degree to which  
187 variation across this dataset could be attributed to tissue-specific variation (here, ovary vs. carcass), species-  
188 specific variation, or neither (residual variation). Using the linear modeling approach adapted from Breschi  
189 and colleagues (2016)<sup>21</sup>, we found the proportion of variance across the dataset attributed to tissue differences  
190 decreased with phylogenetic distance, while the proportion attributed to species difference increased (Fig.  
191 3A-C). In addition, we found that, when comparing ovary and carcass tissues, the Hawaiian drosophilid clade  
192 encompasses the crossover point where variation across species swamps variation across tissues (crossed lines,  
193 Fig. 3A). When comparing across the two species from the *picture-wing* group included in this study, an  
194 average of 45.6% of the variation can be attributed to tissue differences. For the same comparison, 960 genes  
195 were identified as tissue-variable genes (TVGs), defined as residual variation accounting for <25% and a two-  
196 fold increase in variation attributed to tissues than to species (Fig. 3B, S13). In contrast, when comparing  
197 across all twelve Hawaiian drosophilid species studied here, 34.7% of the variation can be attributed to tissue,  
198 with 240 TVGs (Fig. 3B, S13). Across different clades of comparisons, the number of species-variable genes  
199 (SVGs) remains relatively stable (from 304 to 260, Fig. 3B).

200 We then leveraged the results of this linear modeling approach across all twelve species to perform an  
201 additional screen for genes that are consistently upregulated in ovaries across species. We compared the  
202 proportion of variation explained by tissue for each homology group to the average log<sub>2</sub> fold change from the  
203 results of our differential gene expression analysis (Fig 3D). This comparison allowed us to identify genes  
204 that fall above our threshold for TVGs that are also upregulated in the ovary (Fig 3E). This group of genes  
205 includes many of the same members as the core ovary genes (e.g. *nanos* and *swallow*), as well as several new  
206 candidates (e.g. *singed*).

207 To test the importance of tissue identity, we repeated the same analysis comparing variation across species  
208 and tissues using the head in place of the ovary. Consistent with what we describe for the ovary and carcass,  
209 as phylogenetic distance increases the proportion of variation across tissues decreases while variation across  
210 species increases. In contrast to the above findings, however, for the head and carcass far less of the variation  
211 in gene expression can be attributed to tissue differences (Fig. S14). For these tissues, the crossover point  
212 between total proportion of variation occurs roughly at the distance separating the two *picture-wing* species.

213 To verify these results were not driven by the species *S. varia*, which had the most distinct expression patterns  
214 of all species, we repeated these analyses excluding this species and recovered largely equivalent results (Fig.  
215 S15). To compare our findings to those that would be recovered using a more typical pairwise approach,  
216 we repeated the linear modeling analysis on ovary and carcass data using every pairwise combination of  
217 the twelve species. We recovered the same trend of decreasing contribution of tissue-level variation with  
218 increasing phylogenetic distance, and observed that the variance in mean proportion attributed to either  
219 species- or tissue-level differences increased as well (Fig. S16).



### 220 3.3 Identifying gains and losses of ovary bias across genes and the phylogeny

221 While many ovary-specific transcripts belong to the cohort of core ovary genes, on average 75.4% of transcripts  
222 are upregulated in the ovaries of one or several species, but not consistently across ten or more of the species  
223 studied here (Fig 2B-C). This is suggestive of many evolutionary gains and losses of ovary-specific expression  
224 of genes. We characterized the evolution of these gains and losses using an ancestral state reconstruction  
225 approach. First we quantified expression bias between tissues as the ratio of read counts<sup>7</sup>, then reconstructed  
226 the value of this continuous trait for each gene (defined using homology groups) at each node of the estimated  
227 species tree (Fig. S3). We then calculated the scaled change of expression bias along each branch, which  
228 allowed us to describe how relative expression values between tissues had changed the course of evolutionary  
229 time (Fig 4A). Visualizing the distribution of scaled changes by genes shows that most scaled changes are  
230 small and centered around zero, representing little change in gene expression bias between tissues (Fig.  
231 4B-C).

232 Using this dataset of scaled changes across genes and branches, we identified branches for which the direction  
233 of tissue bias had changed (e.g. from higher expression in the ovary than in the carcass to lower, or vice  
234 versa). Visualizing this dataset according to branches reveals that the majority of these changes in bias are  
235 located on the root and terminal branches, rather than internal branches (Fig 4D-E). This is likely because  
236 internal branches for this rapid radiation tend to be very short; even when scaling evolutionary changes  
237 to branch length, it is less probable to experience a shift to and from ovary-biased expression on a short  
238 branch than a long branch. Visualizing the distribution of genes by ancestral and descendant values allows  
239 us to identify shifts in bias which represent the largest swings in expression values (Fig. 4F, points a-d).  
240 Highlighting the top two such shifts in both directions, we identify four example genes which acquired or lost  
241 ovary-specific expression in the phylogeny of Hawaiian Drosophilidae. In the case of *FMRFaR* and *GABA*, a  
242 few Hawaiian species have gained ovary-biased expression of these genes, while most species and the ancestral  
243 state indicate non-ovary bias (Fig. 4Fa-b). In the case of *vilya* and the unnamed gene *CG9109*, each shows  
244 a pattern where one species has lost ovary bias from a biased ancestral state (Fig. 4Fc-d).

245 Repeating the same analysis using the head in place of the ovary revealed a set of evolutionary gains and  
246 losses in head-specific expression (Fig. S17). Identifying the top four changes in head expression shows gains  
247 and losses of head expression in the genes *hiro*, *stil*, *Jhe*, and, consistent with the ovary, *vilya*. In the case of  
248 the latter, these results may be driven by substantial changes in expression of *vilya* in carcass tissues across  
249 species, resulting in major differences in both ovary and head-biased expression.

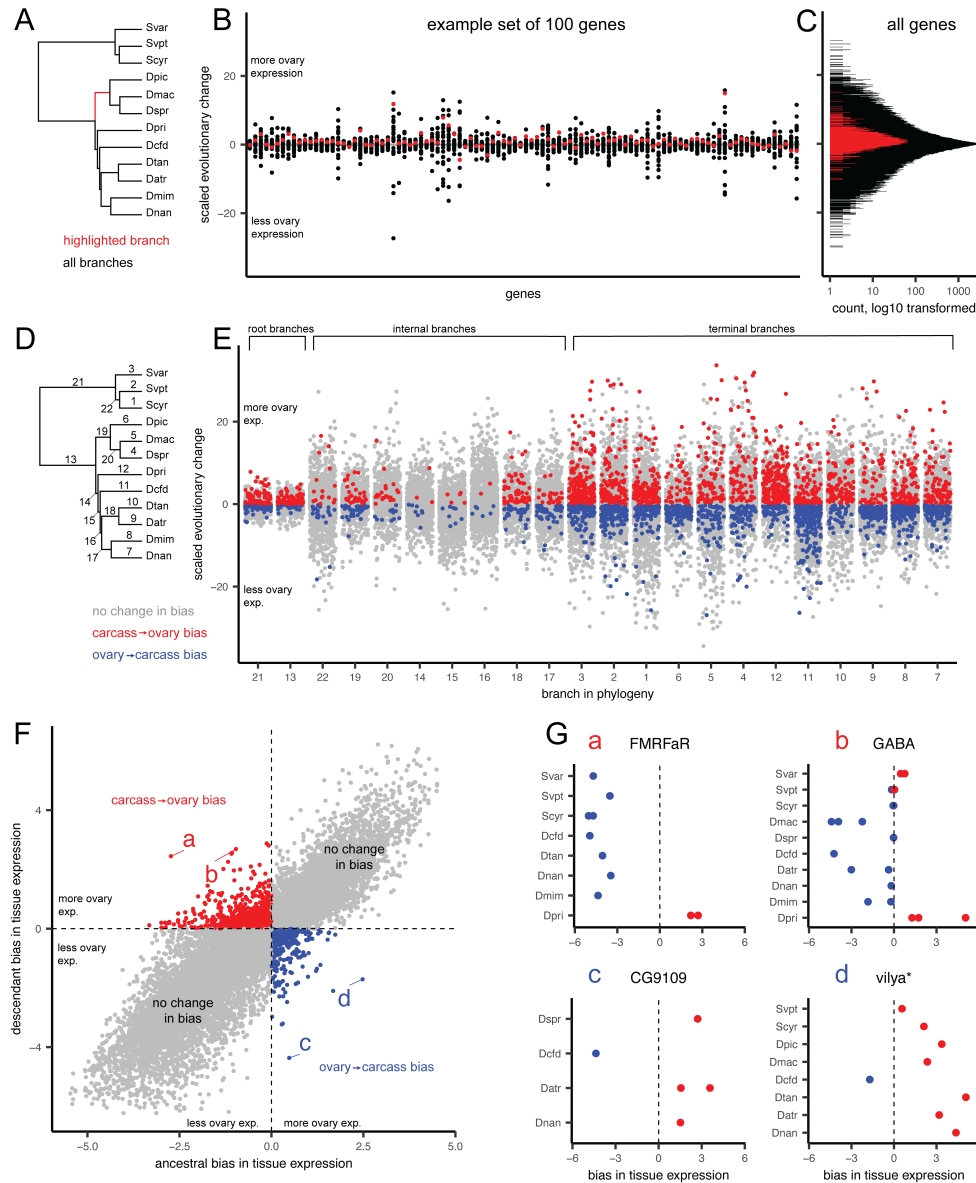


**Figure 4: Identifying genes that have gained and lost ovary-biased expression across the phylogeny.** A, The phylogeny of the twelve species studied here, highlighting one example branch of the 22 for which we inferred the scaled evolutionary change in expression bias. B, The distribution of changes, grouped by gene, for 100 randomly selected genes, defined by homology group. Each point represents one of the 22 branches from A, with the red point corresponding to the highlighted branch from that panel. C, The distribution, log<sub>10</sub> transformed, of scaled genes across all branches and all genes. Changes on the highlighted branch in red. D, The phylogeny with all 22 branches numbered. E, The distribution of changes, grouped by branch, with random jitter on the x-axis within each group. Points colored according to the qualitative change in bias, either from more expression in ovary than carcass to less (blue), the reverse (red), or no change in overall bias (gray). F, The distribution of ancestral and descendant values, showing the two quadrants that represent qualitative changes in bias. Points that represent large swings in expression within those quadrants are labeled a-d. G, The four genes with large swings from F, showing the expression bias for each transcript colored according to more expression in the ovary (red) or carcass (blue). Panels annotated with the gene symbol from the *D. melanogaster* sequences in the same homology group, with the exception of *vilya*\*, which was annotated using a direct BLAST search since no *D. melanogaster* sequence was present in that group.

### 250 3.4 Genes with a strong correlation of expression evolution

251 We tested the estimated evolutionary changes in expression bias for evidence of correlated expression evo-  
252 lution between genes. For every gene represented across all species, we performed a pairwise comparison of  
253 changes in expression bias, using as data points the scaled change in ovary bias on the 22 branches in the  
254 phylogenetic tree. This resulted in 1,306,449 pairwise measures of evolutionary correlation between genes.  
255 Because the number of gene pairs being compared is much larger than the number of values used to esti-  
256 mate correlation, this method has the potential to produce many spurious correlations<sup>7</sup>. To test the degree  
257 to which the correlations observed here reflect known biological interactions between genes, we compared  
258 these measures to reported protein and genetic interactions between genes, using the database of published  
259 genetic experiments in *D. melanogaster*, available at <http://flybase.org>. We found that the mean correlation  
260 coefficient for genes that are known to physically interact as proteins was higher than for genes with no or  
261 unknown interaction (p-value= $<0.001$ , Fig. 5A). This indicates that even with a relatively small number  
262 of observations, there is sufficient information in the matrix to detect biological signal between gene pairs.  
263 These results were calculated based on the correlation in expression bias between the ovary and carcass.  
264 However, following the same procedure using correlations in changes in head-biased expression showed no  
265 significant difference between the two groups (p-value=0.256, Fig. S18), suggesting the strength of this signal  
266 may be dependent on the tissues being compared.

267 We also found that genes known to interact genetically have a significantly higher mean correlation than  
268 genes with no or unknown genetic interactions (unknown vs. enhancement p-value  $<0.001$ , unknown vs. sup-  
269 pression= $<0.001$ , Fig. 5B). Comparing genes with known genetic enhancement and suppression interactions  
270 to each other showed no significant difference (p-value=0.497). However, for genetic interactions, the range  
271 of correlation coefficients was higher in the group of no or unknown interactions (Fig. 5B). This indicates  
272 that, while the average correlation of expression evolution might be higher for interaction partners, stronger  
273 positive and negative correlations exist between pairs of genes which do not interact, or for which interactions  
274 have not yet been tested.

275 As evidence of this, we tested whether the network inferred based on strong correlation of expression evolution  
276 was consistent with known interaction partners from *D. melanogaster*. We selected as an example the gene  
277 yolk-protein gene family, which are known to be expressed in the reproductive system, among other tissues<sup>49</sup>  
278 (Fig. 5C). We found eight distinct homologous gene groups, comprising 14 unique *D. melanogaster* parent  
279 genes, that had a strong evolutionary correlation with yolk-protein genes (absolute coefficient greater than  
280 0.825, Fig. 5D). None of these correlated genes correspond to those listed on FlyBase<sup>50</sup> as having known  
281 interactions with yolk-protein genes in *D. melanogaster* (Fig. 5E). We consider these strong evolutionary  
282 correlations to be a set of new predictions about evolutionary and genetic relationships between genes which  
283 can be tested in wild and laboratory model species of *Drosophila*. The dataset of pairwise correlation  
284 coefficients can be visualized and interrogated at the accompanying data visualization for this manuscript  
285 ([https://github.com/shchurch/hawaiian\\_fly\\_dataviz\\_2021](https://github.com/shchurch/hawaiian_fly_dataviz_2021)).

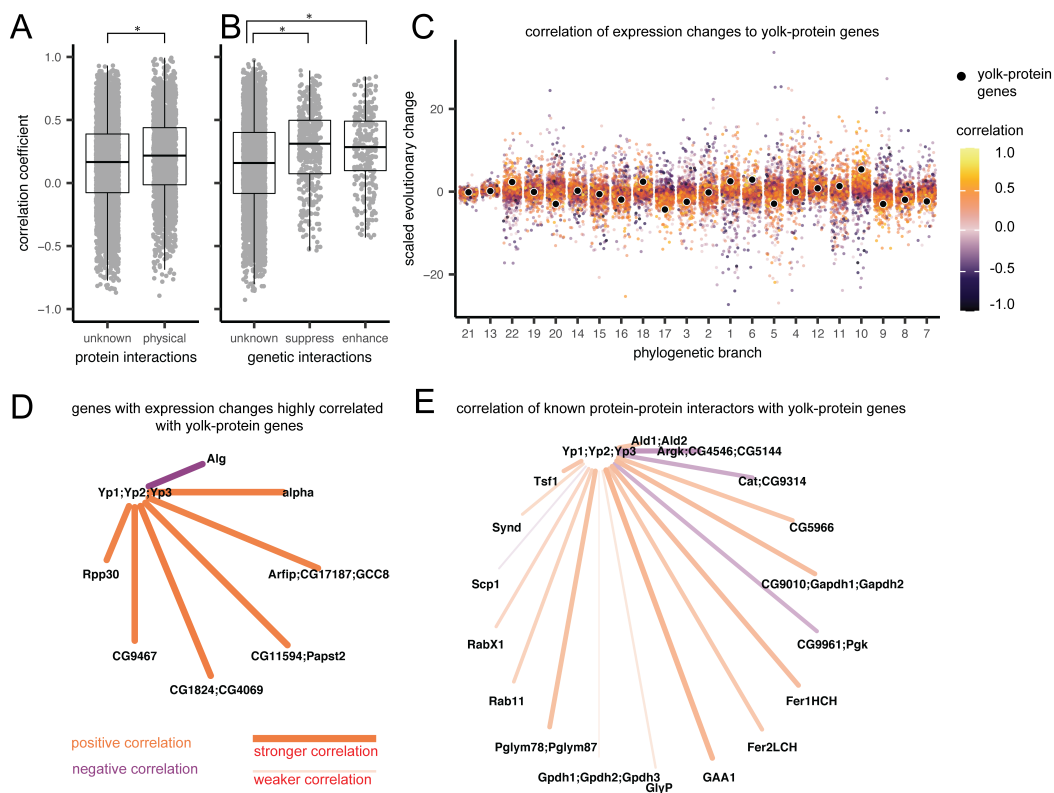


**Figure 5: Estimating pairwise correlation coefficients across genes reveals new networks of correlated expression evolution.** A-B Comparison of the distribution of Pearson's correlation coefficients based on ovary-biased expression evolution between genes. Asterisks indicate a significant t-test comparison. A, Genes with no or unknown protein-protein interactions compared to those with reported interactions in FlyBase<sup>50</sup> (p-value= $<0.001$ ). B, Correlation comparison between genes with no or unknown genetic interactions and those reported to have enhancement or suppression interactions in FlyBase (unknown vs. enhancement p-value= $<0.001$ ; unknown vs. suppression= $<0.001$ ; enhancement vs. suppression= $=0.497$ ). C, Each point represents a scaled change in expression bias, colored by Pearson's correlation coefficients relative to one example gene-family, the yolk-protein genes (black points), arranged by phylogenetic branch (numbers shown in Fig. 4D). Yellow=strong positive correlation, purple=strong negative correlation. D, The network of strong correlation partners (absolute correlation  $> 0.825$ ) with the yolk-protein genes, colored by the direction of correlation. Stronger correlations are shown by brighter colors, and thicker, shorter lines. Nodes are annotated with the gene symbols from the *D. melanogaster* sequences from that homology group. E, The correlation between known protein-protein interaction partners<sup>50</sup> with the yolk-protein genes.

## 286 4 Discussion

287 The results of this study show the importance of placing any comparison of gene expression across species  
 288 in an evolutionary context. When making comparisons that involve model organisms for the study of  
 289 development and disease, this means identifying the crossover point at which variation between species  
 290 begins to swamp variation across the tissues or treatments in question. In such comparisons, the possibility  
 291 that any individual gene may show a divergent pattern of expression from the model organism increases  
 292 substantially. This study provides evidence that confirms we should expect variation in gene expression to  
 293 increase with the phylogenetic distance separating the species being compared. In addition, our results using  
 294 ovary and head expression data show that our expectation should also depend on the identity of the tissues

295 being compared. Our dataset demonstrates that for some tissues, like the fly head, this crossover point may  
296 be met even when comparing between two relatively closely related species.

297 Despite substantial variation across species, we identified core suites of ovary- and head-expressed genes  
298 that have maintained conservation of expression patterns over millions of years of evolution. The core  
299 ovary genes include some of the most well-studied genes in relation to *D. melanogaster* oogenesis, such as  
300 *nanos* and *oskar*, as well as many genes that have yet to be studied in depth (e.g. unnamed genes such  
301 as *CG3430*). We provide the full list of core ovary and head genes as a reference against which future  
302 genetic studies may be informed and compared (Tables S6-S7). Furthermore, the existence of these suites of  
303 genes suggests that equivalent groups are likely to exist within the many gene expression atlases currently  
304 being published<sup>51,52</sup>. New technologies such as single-cell RNA sequencing that use global signatures of gene  
305 expression to identify cells are ripe for interspecific comparisons that may reveal evolutionarily conserved  
306 gene modules<sup>53</sup>. Developing robust comparative methods for comparing these atlases across species has  
307 the potential to reveal ancestral expression patterns in cells and organs, as well as pinpoint important  
308 evolutionary shifts in expression regulation.

309 Our results indicate that genes known to interact, both physically as the proteins they encode and through  
310 genetic enhancement and suppression, likely experience more correlated changes in expression than would  
311 be expected for genes chosen at random. However, we also find the difference in mean correlation between  
312 these groups to be relatively small, and dependent on the context of the tissue in question. One possible  
313 explanation for this finding is that interactions between genes with strong correlations of expression evolution  
314 have yet to be described. We provide an interactive tool to explore highly correlated genes that can inform  
315 future genetic studies in *D. melanogaster* and other related species ([https://github.com/shchurch/hawaiian\\_fly\\_dataviz\\_2021](https://github.com/shchurch/hawaiian_fly_dataviz_2021)). Another possibility we consider likely is that interactions between genes represent only  
316 one factor among many that dictate the probability of correlated changes in expression. We hypothesize  
317 that other features, such as shared regulatory or chromatin architecture, will also influence evolutionary  
318 correlation of expression.  
319

320 As more studies undertake phylogenetic comparisons of functional genomic data, new factors that influence  
321 the evolutionary associations between genes are likely to be revealed<sup>7</sup>. The strength of these phylogenetic  
322 comparisons will depend in part on comparing across a sufficient number of taxa such that there are multiple  
323 branches on which to calculate and compare evolutionary changes. However, even as functional genomic data  
324 become more accessible for more species, the number of features being compared (e.g. thousands of genes) will  
325 likely continue to outnumber the number of evolutionary observations (e.g. changes along branches)<sup>7</sup>. One  
326 encouraging result from this study is that, using our matrix of gene expression changes along 22 branches, we  
327 find sufficient information to detect the biological signal associated with physical and genetic interactions.  
328 While this is true, we assume that some fraction of the correlations that we report here represent false  
329 positives, and that the strength of correlation of these genes would decrease with the addition of more taxa  
330 to the comparison. For this reason we present the correlation matrix as a set of hypotheses to be tested in  
331 future studies using additional lines of evidence.

332 One outstanding challenge in expression evolution is the quality of the references available against which  
333 RNA reads can be mapped<sup>48</sup>. In this study we account for the statistical noise in our data by averaging  
334 expression values over groups of homologous genes, as identified by sequence similarity to high quality refer-  
335 ence genomes. This approach has the advantage of accounting for problems associated with fragmentation of  
336 genes in transcriptome assembly. However, it comes at the cost of averaging over possible biological variation  
337 in expression between genes from the same gene family. The strong concordance of our results with published  
338 records from *D. melanogaster* suggests that the approach we have used here is robust for our dataset. How-  
339 ever, as the quality and accessibility of genomes from diverse species continue to increase, future studies will  
340 likely be able to compare directly between orthologous genes without needing to account for fragmentation.  
341 For those future studies, a phylogenetic comparative approach like the one used here and elsewhere<sup>8</sup> can  
342 serve as an analytical framework to move expression comparisons beyond pairwise comparisons.

343 One goal of evolutionary developmental biology is to identify changes in developmental mechanisms that  
344 underlie phenotypic differences<sup>12</sup>. Many studies approach this by identifying phenotypic variation between  
345 species and then searching for differences in gene content or expression using one or several emerging model  
346 organisms in the lab<sup>12</sup>. To narrow down the field of search, this approach often requires `_a priori_`

347 knowledge of candidate genes, gained from developmental research in related models or other methods of  
348 filtering the genome. Furthermore, because these approaches usually lack global measurements of gene  
349 expression variation across species, identifying an expression difference does not always constitute a smoking  
350 gun<sup>6</sup>. For example, observing a difference in candidate gene expression between taxa would not be unexpected  
351 if we frequently observe differences of that magnitude between genes chosen at random. An alternative  
352 approach, as demonstrated here, is to characterize all the evolutionary changes in expression across the  
353 transcriptome, and then identify the changes that are significantly associated with traits of interest<sup>9</sup>. As  
354 expression data become available from an ever wider array of species, this “evolutionary screen” approach  
355 becomes increasingly possible. One advantage of this approach is that it may reveal associations that would  
356 otherwise escape detection when comparisons are centered on model organisms; for example, when genes,  
357 traits, or processes happen to not be present in our laboratory model species<sup>10</sup>. By leveraging phylogenetic  
358 comparative methods on high-dimensional functional genomic data, the objective of connecting genomic  
359 variation to developmental mechanisms and phenotypic differences will be accelerated.

## 360 5 Methods

### 361 5.1 Field collection

362 Specimens used for transcriptome sampling were caught on the Hawaiian islands between May of 2016 and  
363 May of 2017. Specimens were caught using a combination of net sweeping and fermented banana-mushroom  
364 baits in various field sites on the Hawaiian islands of Kaua’i and Hawai’i (see Table S1 for locality data).  
365 Field collections were performed under permits issued by the following: Hawai’i Department of Land and  
366 Natural Resources, Hawai’i Island Forest Reserves, Kaua’i Island Forest Reserves, Koke’e State Park, and  
367 Hawai’i Volcanoes National Park. Adult flies were maintained in the field on vials with sugar media and kept  
368 at cool temperatures. They were transported alive back to Cambridge, MA where they were maintained on  
369 standard *Drosophila* media at 18°C. Samples were processed for RNA extraction between 5 and 31 days after  
370 collecting them live in the field (average 10.8 days, see Table S1). One species, *Scaptomyza varia*, was caught  
371 in the field before the adult stage by sampling rotting *Clermontia sp.* flowers (the oviposition substrate).  
372 For this species, male and female adult flies emerged in the lab, and were kept together until sampled for  
373 RNA extraction.

### 374 5.2 Species identification

375 Species were identified using dichotomous keys<sup>54–58</sup>, when possible. Many keys for Hawaiian Drosophili-  
376 dae are written focusing on male specific characters (e.g. sexually dimorphic features or male genitalia)<sup>56</sup>.  
377 Therefore, for species where females could not be unambiguously identified by morphology, we verified their  
378 identity using DNA barcoding. When males were caught from the same location, we identified males to  
379 species using dichotomous keys and matched their barcode sequences to females included in our study. We  
380 also matched barcodes from collected females to sequences previously uploaded to NCBI<sup>59–61</sup>.

381 The following dichotomous keys were used to identify species: for *picture-wing* males and females, Magnacca  
382 and Price (2012)<sup>54</sup>; for *antopocerus* males, Hardy (1977)<sup>55</sup>; for *Scaptomyza*, Hackman (1959)<sup>56</sup>; for species  
383 in the *mimica* subgroup of MM, O’Grady and colleagues (2003)<sup>57</sup>; for other miscellaneous species, Hardy  
384 (1965)<sup>58</sup>.

385 For DNA barcoding, DNA was extracted from one or two legs from male specimens using the Qiagen DNeasy  
386 blood and tissue extraction kit, or from the DNA of females isolated during RNA extraction (see below). We  
387 amplified and sequenced the cytochrome oxidase I (COI), II (COII) and 16S rRNA genes using the primers  
388 and protocols described in Sarikaya and colleagues (2019)<sup>40</sup>.

389 For barcode matching, we aligned sequences using MAFFT, version v7.475<sup>62</sup>, and assembled gene trees  
390 using RAxML, version 8.2.9<sup>63</sup>. Definitive matches were considered when sequences for females formed a  
391 monophyletic clade with reference males or reference sequences from NCBI; see Table S2.

392 Female *D. primaeva*, *D. macrothrix*, *D. sproati*, and *D. picticornis* could be identified unambiguously using  
393 dichotomous keys. Female *D. atroscutellata*, *D. nanella*, *D. mimica*, *D. tanythrix*, *S. cyrtandrae*, *S. varipicta*,  
394 and *S. varia* were identified by matching barcodes to reference sequences from NCBI, reference males, or  
395 both. For the female *haleakalae* fly used in this study, no male flies were caught in the same location as these  
396 individuals, and no other sequences for *haleakalae* males on NCBI were an exact match with this species.  
397 Given its similar appearance to *Drosophila dives*, we are referring to it here as *Drosophila* cf *dives*, and we  
398 await further molecular and taxonomic studies of this group that will resolve its identity.

### 399 5.3 Sampling strategy

400 The target number of mature, healthy female flies per species was four, with three intended for dissection  
401 and species-specific expression libraries and one intended as a whole-body reference library (Fig. 1). When  
402 four such individuals were not available, a reference library was assembled by combining the tissue-specific  
403 libraries from one of the other individuals. This was the case for the following species: *D. sproati*, which  
404 was dissected and had RNA extracted separately from the head, ovaries, and carcass, with RNA combined  
405 prior to library preparation; and *S. varia*, *S. cyrtandrae* and *D. cf dives*, for which RNA was extracted and  
406 libraries prepared for separate tissues, and raw reads were combined after sequencing.

407 For the other eight species, sufficient individual females were available such that reads for transcriptome  
408 assembly were sequenced from a separate individual. In these cases one entire female fly was dissected and  
409 photographed to assess whether vitellogenic eggs were present in the ovary, and all tissues were combined in  
410 the same tube and used for RNA extraction. Library preparation failed for one individual *D. atroscutellata*  
411 fly, as well as two tissue-specific libraries: one head sample from *D. mimica*, and one head sample from *D.*  
412 *sproati*.

### 413 5.4 Dissection and RNA sequencing

414 Female flies were anesthetized in 100% ethanol and were dissected in a 1x phosphate-buffered saline solution.  
415 The ovary was separated from the abdomen, and the head was separated from the carcass. Photographs  
416 of each tissue were taken, and tissues were moved to pre-frozen eppendorf tubes, kept in dry ice, and  
417 immediately transported to a -80°C freezer. Dissections were performed as quickly as possible to prevent  
418 RNA degradation. Samples were stored at -80°C for between 90 and 336 days before RNA extraction (average  
419 281.9 days, see Table S1).

420 RNA was extracted from frozen samples using the standard TRIzol protocol ([http://tools.thermofisher.com/content/sfs/manuals/trizol\\_reagent.pdf](http://tools.thermofisher.com/content/sfs/manuals/trizol_reagent.pdf)). One mL of TRIzol was added to each frozen sample, which  
421 were then homogenized using a sterile motorized mortar. The recommended protocol was followed without  
422 modifications, using 10 µg of glycogen, and resuspending in 20µL RNase-free water-EDTA-SDS solution.  
423 DNA for subsequent barcoding was also extracted using the phenol-chloroform phase saved from the RNA  
424 extraction.

426 RNA concentration was checked using a Qubit fluorometer, and integrity was assessed with a Agilent TapeS-  
427 tation 4200. RNA libraries were prepared following the PrepX polyA mRNA Isolation kit and the PrepX  
428 RNA-Seq for Illumina Library kit, using the 48 sample protocol on an Apollo 324 liquid handling robot in  
429 the Harvard University Bauer Core Facilities. Final library concentration and integrity were again assessed  
430 using the Qubit and TapeStation protocols.

431 Samples intended for transcriptome assembly were sequenced on an Illumina HiSeq 2500, using the standard  
432 version 4 protocol, at 125 base pairs of paired-end reads. Samples intended for tissue-specific expression  
433 analyses were sequenced on an Illumina NextSeq 500, using a high output flow cell, at 75 base pairs of  
434 single-end reads. A table of total read counts for each library can be found in Tables S3-S4. To account  
435 for any possible batch effects across separate rounds of sequencing, each sequencing run was performed with  
436 one or several overlapping samples. Principle component analysis of these libraries showed variation between  
437 sequencing runs to be negligible relative to variation between tissue and individual (see Results and Fig.  
438 S7).

## 439 5.5 Transcriptome assembling and expression mapping

440 Transcriptome assembly and expression mapping was performed using the agalma pipeline, version 2.0.0<sup>47</sup>.  
441 For the twelve reference transcriptomes, reads from separate rounds of sequencing were concatenated and  
442 inserted into the agalma catalog. Further details of transcriptome assembly and homology assessment are  
443 included in our previous manuscript<sup>44</sup>.

444 Each tissue-specific expression library was mapped to the corresponding reference transcriptome using the  
445 ‘expression’ pipeline in agalma, which uses the software RSEM to estimate gene and isoform count levels  
446 from RNAseq data<sup>64</sup>. The agalma pipeline also includes steps to catalog the species, tissue type, and run  
447 information, which were exported as a single JavaScript object notation (JSON) file. This file is available in  
448 the GitHub repository in the directory `analysis/data`.

## 449 5.6 Phylogenetic analysis

450 The phylogenetic methods for inferring homology, orthology, and estimating gene and species trees are the  
451 same as those described in our previous manuscript<sup>44</sup>. Genetrees were additionally annotated with the  
452 software Phyldog<sup>65</sup>.

## 453 5.7 Annotating transcripts by sequence similarity

454 We leveraged the close relationship of these species to species of *Drosophila* with well-annotated genomes to  
455 annotate the transcripts considered here. For each transcript in the reference transcriptome, we performed  
456 four comparisons of sequence similarity using local BLAST: [1] comparing nucleotide transcript sequences to  
457 nucleotide sequences from *D. melanogaster* (blastn), [2] comparing translated nucleotide sequences to protein  
458 sequences of *D. melanogaster* (blastx), [3] comparing nucleotide sequences to a database of nucleotide se-  
459 quences from *D. melanogaster*, *D. virilis*, and *D. grimshawi* (blastx), and [4] comparing translated nucleotide  
460 sequences to a database of protein sequences from the same three species (blastn). For downstream analyses,  
461 we prioritized annotations from the second comparison, but we provide all sequence similarity reports in the  
462 GitHub repository under the directory `analysis/BLAST`.

463 To annotate homolog groups as defined by the homology inference step of agalma, we extracted the name  
464 and sequence ID from all *D. melanogaster* sequences in the group.

## 465 5.8 Normalization and differential gene expression

466 Transcript count tables were imported into R using the agalmar package, version 0.0.0.9000. Differential gene  
467 expression analysis was performed using the package DESeq2, version 1.34.0. For these analyses we used only  
468 one sequencing run per library, thereby excluding duplicate sequencing runs. Analyses of differential gene  
469 expression were calculated using the default approaches in DESeq2 for estimating size factors, dispersions,  
470 and calculating log<sub>2</sub> fold-change and p-values (Fig. S2A). Both individual and tissue were considered in the  
471 design formula. Transcripts were considered differentially expressed at a significance threshold of 0.01.

472 We identified a cohort of core ovary-specific genes by first identifying a parent gene for each transcript using  
473 a sequence similarity search against *D. melanogaster* (Fig. S2A). We then identified parent genes that had  
474 at least one transcript significantly differentially upregulated in the ovary of more than ten of the twelve  
475 species. Because multiple transcripts may match to a single parent-gene, core ovary-specific parent genes  
476 may include transcripts that are also not differentially upregulated in the ovary, as long as at least one  
477 transcript is for more than ten out of twelve species. This may be the case when transcripts are artificially  
478 fragmented during reference transcriptome assembly, or when sequence-similar transcripts have biologically  
479 distinct expression levels.

## 480 5.9 Comparison of expression to *D. melanogaster*

481 We compared our differential gene expression results to a reference database of tissue expression from *D.*  
482 *melanogaster*, known as the FlyAtlas2<sup>29</sup>. We downloaded this reference in July of 2021, from [http://motif.gla.ac.uk/downloads/FlyAtlas2\\_21.04.18.sql](http://motif.gla.ac.uk/downloads/FlyAtlas2_21.04.18.sql). This dataset provides data on transcript abundance and tissue  
483 enrichment, including for female ovaries. Tissue enrichment is calculated using the same methods as in the  
484 FlyAtlas2 web browser, defined as the fragments per kilobase of transcript per million mapped reads (FPKM)  
485 for a given tissue divided by that value for the reference tissue (here, female whole body), with a pseudocount  
486 of two counts added to empty values to avoid division by zero. We considered a FlyAtlas gene to be enriched  
487 in the ovary, comparable to our data, if the ovary was the maximum enrichment value across all tissues  
488 excluding the head, brain, and eye tissues, as these were separated in our RNASeq procedure (Fig. S2A).  
489 We considered a FlyAtlas gene to be head enriched if either the head, brain, or eye were the maximum  
490 enrichment value, excluding the ovary.  
491

## 492 5.10 Transforming data into comparable measurements of expression across 493 species

494 Transcript counts are reported in transcripts per million (TPM), but this measurement is known to not  
495 be directly comparable across species due to differences in reference transcriptome size<sup>7,8</sup>. Therefore, we  
496 normalized TPM by species using the procedure described by Munro and colleagues (2021)<sup>8</sup>, where TPM  
497 values are multiplied by the number of genes in the reference, and this value is divided by  $10^4$  (Fig. S2B).  
498 TPM10k values were natural-log transformed.

499 An additional challenge when working with reference transcriptomes is the presence of fragmented transcripts  
500 created during the assembly process<sup>48</sup>. This fragmentation can result in noise in estimating the amount of  
501 transcript as reads are differentially mapped to these fragments. To reduce the impact of this noise on our  
502 analysis, we undertook a novel approach where transcripts were grouped according to inferred homology  
503 as estimated by the agalma pipeline using an all-by-all BLAST approach (Fig. S2B). For each sequenced  
504 library, we then found the average count value across all transcripts from the same homology group (see  
505 Table S5 for statistics on homology group composition). For each species-tissue pair, we then averaged this  
506 value across all biological replicates, here replicate individuals.

## 507 5.11 Linear modeling

508 We performed linear modeling to calculate the relative contribution of tissue- and species-level differences  
509 to variation in gene expression (Fig. S2B), following the approach of Breschi and colleagues (2016)<sup>21</sup>. These  
510 analyses were performed separately on datasets of ovary vs. carcass and head vs. carcass expression. Using  
511 the ANOVA script provided at <https://github.com/abreschi/Rscripts/blob/master/anova.R>, we built  
512 a linear model for each gene that accounts for the contribution of the organ, species, and any residual error.  
513 We then calculated the relative proportion of each factor divided by the total sum of squares for all factors.  
514 We identified groups of highly variable genes, using the same metrics defined by Breschi and colleagues  
515 (2016)<sup>21</sup>, as any gene for which either tissues or species explains at least 75% of the variance. Species  
516 variable genes (SVGs) were defined as highly variable genes whose relative variation was two-fold greater  
517 across species than tissues (vice-versa for tissue variable genes, TVGs).

518 We performed these linear model analyses over four nested clades: a clade containing two *picture-wing* species  
519 (*D. sproati* and *D. macrothrix*); a clade containing the four *picture-wing-Nudidrosophila-Ateledrosophila*  
520 species in this study; a clade containing the nine Hawaiian *Drosophila* species in this study; and a clade of  
521 all 12 Hawaiian *Drosophila* and *Scaptomyza* species in this study. We repeated these analyses excluding the  
522 species *S. varia*, which showed the lowest similarity in expression to the other eleven species. To compare  
523 our analysis to the more typical approach undertaken, we also performed these analyses on all pairwise  
524 combinations of these twelve species.

## 5.12 Reconstructing evolutionary history of differential expression

We calculated tissue bias as the ratio of counts in TPM10k for each tissue (ovary and head) to the reference tissue<sup>7</sup>, here the carcass (Fig. S3A). We subsequently performed the same transformation steps described above, averaging over ratios from the same homology group and across biological replicates, to calculate average expression bias per homology group per library. To avoid division by zero, we added a pseudocount of 0.01 to each TPM10k value. Ratio values were natural-log transformed so that positive values indicate enrichment in the tissue of interest relative to the reference tissue, negative values indicate the opposite, and values of zero indicate equivalent expression.

We reconstructed the evolutionary history of tissue bias for each homology group using the species tree published in Church and Extavour, 2021<sup>44</sup>, based on the same reference transcriptome data (Fig. S2C). First, we calibrated the tree estimated using IQtree (Fig 1A of that publication) to be ultrametric using the R function `chronos` in the package `ape`, version 5.6.2 (using a correlated model and a lambda value of 1). We then subset this tree to only include tips for which expression data was available, and annotated this tree to be able to identify specific branches and nodes in ancestral state reconstruction analyses.

Ancestral expression bias values were estimated with the R package `Rphylopars`, version 0.3.8, using the fast ancestral state reconstruction algorithm based on Ho and Ané, 2014<sup>66</sup> (Fig. S3A). Tips for which expression data were not available were dropped from each reconstruction, and ancestral state reconstruction was only performed when more than three tips had data. Following ancestral state reconstruction, we calculated the scaled change as the difference between the value at the ancestral and descendant nodes, divided by the length of the branch. Scaled changes were compared between homology groups by identifying equivalent branches as those that share the same parent and child node, following the procedure described in Munro and colleagues (2021)<sup>8</sup>. We identified qualitative changes in expression bias as changes that resulted in a ratio changing from negative to positive values or vice versa.

## 5.13 Estimating correlated evolution of expression across genes

For each homology group that had representation across all twelve species, we calculated pairwise Pearson's correlation coefficients by comparing scaled changes in expression bias across equivalent branches (Fig. S3B). For the twelve-species phylogeny, this meant each correlation coefficient was calculated using 22 individual data points (branches). This resulted in a correlation matrix of 1,306,449 pairwise comparisons of evolutionary correlation.

We compared this correlation network to data on protein interactions and genetic interactions downloaded from <http://flybase.org> in July, 2021. These data include pairwise observations of genetic enhancement and suppression interactions between parent genes in *D. melanogaster*. These interactions were matched to pairwise correlation coefficients by identifying the corresponding homology group for each *D. melanogaster* parent gene ID (more than one parent gene may fall into the same homology group).

We tested whether correlation coefficients for known genetic interaction partners were higher than in genes with unknown interactions using two-sample t-tests. In each test we compared the coefficients for either enhancement or suppression interactions to a random sample of 5000 coefficients for which interactions are unknown. We repeated these t-tests 100 times using different random samples, and report the maximum p-value observed. We also compared the distribution of enhancement and suppression interaction coefficients to each other using a single t-test.

Strong correlations for the visualization of co-evolutionary networks were selected using a threshold correlation coefficient of 0.825.

## 6 Data Availability

All data, results, and code for this manuscript are available at GitHub, under the repository `shchurch/hawaiian_drosophilidae_expression_2021`, commit `67d8e6f`. The code to perform all

570 agalma commands was performed in clean anaconda environment, installed following the instructions  
571 at <https://bitbucket.org/caseywdunn/agalma>. All R commands were performed with a fresh install  
572 of R, and the session information including all package versions is available in the GitHub repository  
573 under the file `r_session_info.txt`. The code to generate all plots as well as the text of this manuscript  
574 is available in several R scripts and Rmarkdown files at the same location. The resulting correlation  
575 matrix can be interactively visualized and queried at the accompanying data visualization for this paper  
576 ([https://github.com/shchurch/hawaiian\\_fly\\_dataviz\\_2021](https://github.com/shchurch/hawaiian_fly_dataviz_2021)).

## 577 **7 Acknowledgments**

578 This work was partially supported by National Science Foundation Graduate Research Fellowship Program  
579 DGE1745303 to SHC, National Institutes of Health award R01 HD073499-01 (NICHD) to CGE, and funds  
580 from Harvard University to support SHC and CGE. We thank Didem Sarikaya, Karl Magnacca, and Steve  
581 Montgomery for their field assistance and expertise in Hawaiian fly identification and husbandry. We thank  
582 Kenneth Kaneshiro for the use of his lab space in preparing wild caught specimens. We thank Bruno de  
583 Medeiros, Seth Donoughe, and members of the Dunn and Extavour labs for discussion of ideas.

## 584 **8 Competing Interest**

585 The authors declare no competing interests.

## 586 References

- 587 1. Wang, Z., Gerstein, M. & Snyder, M. RNA-seq: A revolutionary tool for transcriptomics. *Nature Reviews*  
588 *Genetics* **10**, 57–63 (2009).
- 589 2. Ozsolak, F. & Milos, P. M. RNA sequencing: Advances, challenges and opportunities. *Nature Reviews*  
590 *Genetics* **12**, 87–98 (2011).
- 591 3. Van Dijk, E. L., Auger, H., Jaszczyszyn, Y. & Thermes, C. Ten years of next-generation sequencing  
592 technology. *Trends in Genetics* **30**, 418–426 (2014).
- 593 4. McDermaid, A., Monier, B., Zhao, J., Liu, B. & Ma, Q. Interpretation of differential gene expression  
594 results of RNA-seq data: Review and integration. *Briefings in Bioinformatics* **20**, 2044–2054 (2019).
- 595 5. Dunn, C. W., Zapata, F., Munro, C., Siebert, S. & Hejnol, A. Pairwise comparisons across species are  
596 problematic when analyzing functional genomic data. *Proceedings of the National Academy of Sciences* **115**,  
597 E409–E417 (2018).
- 598 6. Church, S. H. & Extavour, C. G. Null hypotheses for developmental evolution. *Development* **147**,  
599 dev178004 (2020).
- 600 7. Dunn, C. W., Luo, X. & Wu, Z. Phylogenetic analysis of gene expression. *Integrative and Comparative*  
601 *Biology* **53**, 847–856 (2013).
- 602 8. Munro, C., Zapata, F., Howison, M., Siebert, S. & Dunn, C. W. Evolution of gene expression across  
603 species and specialized zooids in Siphonophora. *bioRxiv* (2021).
- 604 9. Smith, S. D., Pennell, M. W., Dunn, C. W. & Edwards, S. V. Phylogenetics is the new genetics (for most  
605 of biodiversity). *Trends in Ecology & Evolution* **35**, 415–425 (2020).
- 606 10. Dunn, C. W., Leys, S. P. & Haddock, S. H. The hidden biology of sponges and ctenophores. *Trends in*  
607 *Ecology & Evolution* **30**, 282–291 (2015).
- 608 11. Arias, A. M. *Drosophila melanogaster* and the development of biology in the 20th century. *Drosophila*  
609 **420**, 1–25 (2008).
- 610 12. Jenner, R. A. & Wills, M. A. The choice of model organisms in evo–devo. *Nature Reviews Genetics* **8**,  
611 311–314 (2007).
- 612 13. Yanai, I., Graur, D. & Ophir, R. Incongruent expression profiles between human and mouse orthologous  
613 genes suggest widespread neutral evolution of transcription control. *OmicS: a Journal of Integrative Biology*  
614 **8**, 15–24 (2004).
- 615 14. Lin, S. *et al.* Comparison of the transcriptional landscapes between human and mouse tissues. *Proceed-*  
616 *ings of the National Academy of Sciences* **111**, 17224–17229 (2014).
- 617 15. Gilad, Y. & Mizrahi-Man, O. A reanalysis of mouse ENCODE comparative gene expression data.  
618 *F1000Research* **4**, 1–30 (2015).
- 619 16. Liao, B.-Y. & Zhang, J. Evolutionary conservation of expression profiles between human and mouse  
620 orthologous genes. *Molecular Biology and Evolution* **23**, 530–540 (2006).
- 621 17. Cardoso-Moreira, M. *et al.* Gene expression across mammalian organ development. *Nature* **571**, 505–509  
622 (2019).
- 623 18. Fukushima, K. & Pollock, D. D. Amalgamated cross-species transcriptomes reveal organ-specific propen-  
624 sity in gene expression evolution. *Nature Communications* **11**, 1–14 (2020).
- 625 19. Merkin, J., Russell, C., Chen, P. & Burge, C. B. Evolutionary dynamics of gene and isoform regulation  
626 in mammalian tissues. *Science* **338**, 1593–1599 (2012).
- 627 20. Brawand, D. *et al.* The evolution of gene expression levels in mammalian organs. *Nature* **478**, 343–348  
628 (2011).

- 629 21. Breschi, A. *et al.* Gene-specific patterns of expression variation across organs and species. *Genome*  
630 *Biology* **17**, 1–13 (2016).
- 631 22. Robinson, S. W., Herzyk, P., Dow, J. A. & Leader, D. P. FlyAtlas: Database of gene expression in the  
632 tissues of *Drosophila melanogaster*. *Nucleic Acids Research* **41**, D744–D750 (2013).
- 633 23. Graveley, B. R. *et al.* The developmental transcriptome of *Drosophila melanogaster*. *Nature* **471**,  
634 473–479 (2011).
- 635 24. St. Pierre, S. E., Ponting, L., Stefancsik, R., McQuilton, P. & Consortium, F. FlyBase 102—advanced  
636 approaches to interrogating flybase. *Nucleic Acids Research* **42**, D780–D788 (2014).
- 637 25. Chintapalli, V. R., Wang, J. & Dow, J. A. Using flyatlas to identify better *Drosophila melanogaster*  
638 models of human disease. *Nature Genetics* **39**, 715–720 (2007).
- 639 26. Papatheodorou, I. *et al.* Expression atlas: Gene and protein expression across multiple studies and  
640 organisms. *Nucleic Acids Research* **46**, D246–D251 (2018).
- 641 27. Butler, A., Hoffman, P., Smibert, P., Papalexi, E. & Satija, R. Integrating single-cell transcriptomic  
642 data across different conditions, technologies, and species. *Nature Biotechnology* **36**, 411–420 (2018).
- 643 28. Parisi, M. *et al.* A survey of ovary-, testis-, and soma-biased gene expression in *Drosophila melanogaster*  
644 adults. *Genome Biology* **5**, 1–18 (2004).
- 645 29. Leader, D. P., Krause, S. A., Pandit, A., Davies, S. A. & Dow, J. A. T. FlyAtlas 2: A new version of the  
646 *Drosophila melanogaster* expression atlas with RNA-seq, miRNA-seq and sex-specific data. *Nucleic Acids*  
647 *Research* **46**, D809–D815 (2018).
- 648 30. Kumar, T., Blondel, L. & Extavour, C. G. Topology-driven protein-protein interaction network analysis  
649 detects genetic sub-networks regulating reproductive capacity. *Elife* **9**, e54082 (2020).
- 650 31. Kirilly, D. & Xie, T. The *Drosophila* ovary: An active stem cell community. *Cell Research* **17**, 15–25  
651 (2007).
- 652 32. Jagut, M. *et al.* A mosaic genetic screen for genes involved in the early steps of *Drosophila* oogenesis.  
653 *G3: Genes, Genomes, Genetics* **3**, 409–425 (2013).
- 654 33. Barnett, T., Pacht, C., Gergen, J. P. & Wensink, P. C. The isolation and characterization of *Drosophila*  
655 yolk protein genes. *Cell* **21**, 729–738 (1980).
- 656 34. Kugler, J.-M. & Lasko, P. Localization, anchoring and translational control of oskar, gurken, bicoid and  
657 nanos mRNA during *Drosophila* oogenesis. *Fly* **3**, 15–28 (2009).
- 658 35. Stephenson, E. C., Chao, Y.-C. & Fackenthal, J. D. Molecular analysis of the *swallow* gene of *Drosophila*  
659 *melanogaster*. *Genes & development* **2**, 1655–1665 (1988).
- 660 36. O’Grady, P. & DeSalle, R. Hawaiian *Drosophila* as an evolutionary model clade: Days of future past.  
661 *Bioessays* **40**, 1700246 (2018).
- 662 37. Obbard, D. J. *et al.* Estimating divergence dates and substitution rates in the *Drosophila* phylogeny.  
663 *Molecular Biology and Evolution* **29**, 3459–3473 (2012).
- 664 38. Kambysellis, M. P. *et al.* Pattern of ecological shifts in the diversification of Hawaiian *Drosophila* inferred  
665 from a molecular phylogeny. *Current Biology* **5**, 1129–1139 (1995).
- 666 39. Montague, J. R., Mangan, R. L. & Starmer, W. T. Reproductive allocation in the Hawaiian Drosophili-  
667 dae: Egg size and number. *The American Naturalist* **118**, 865–871 (1981).
- 668 40. Sarikaya, D. P. *et al.* Reproductive capacity evolves in response to ecology through common changes in  
669 cell number in Hawaiian *Drosophila*. *Current Biology* **29**, 1877–1884 (2019).
- 670 41. Church, S. H., Donoughe, S., Medeiros, B. A. de & Extavour, C. G. A dataset of egg size and shape  
671 from more than 6,700 insect species. *Scientific Data* **6**, 1–11 (2019).

- 672 42. Church, S. H., Medeiros, B. A. de, Donoughe, S., Márquez Reyes, N. L. & Extavour, C. G. Repeated  
673 loss of variation in insect ovary morphology highlights the role of development in life-history evolution.  
674 *Proceedings of the Royal Society B* **288**, 20210150 (2021).
- 675 43. Edwards, K. A., Doescher, L. T., Kaneshiro, K. Y. & Yamamoto, D. A database of wing diversity in the  
676 Hawaiian *Drosophila*. *PLoS One* **2**, e487 (2007).
- 677 44. Church, S. H. & Extavour, C. G. Phylotranscriptomics reveals discordance in the phylogeny of Hawaiian  
678 *Drosophila* and *Scaptomyza* (Diptera: Drosophilidae). *bioRxiv* (2021).
- 679 45. McLaughlin, J. M. & Bratu, D. P. *Drosophila melanogaster* oogenesis: An Overview. *Methods in*  
680 *molecular biology (Clifton, NJ)* **1328**, 1–20 (2015).
- 681 46. Hoshino, M., Suzuki, E., Nabeshima, Y.-i. & Hama, C. Hikaru genki protein is secreted into synaptic  
682 clefts from an early stage of synapse formation in *Drosophila*. *Development* **122**, 589–597 (1996).
- 683 47. Dunn, C. W., Howison, M. & Zapata, F. Agalma: An automated phylogenomics workflow. *BMC*  
684 *Bioinformatics* **14**, 1–9 (2013).
- 685 48. Freedman, A. H., Clamp, M. & Sackton, T. B. Error, noise and bias in de novo transcriptome assemblies.  
686 *Molecular Ecology Resources* **21**, 18–29 (2021).
- 687 49. Garabedian, M. J., Shepherd, B. M. & Wensink, P. C. A tissue-specific transcription enhancer from the  
688 *Drosophila* yolk protein 1 gene. *Cell* **45**, 859–867 (1986).
- 689 50. Larkin, A. *et al.* FlyBase: Updates to the *Drosophila melanogaster* knowledge base. *Nucleic Acids*  
690 *Research* **49**, D899–D907 (2021).
- 691 51. Consortium, T. M. & others. Single-cell transcriptomics of 20 mouse organs creates a *Tabula Muris*.  
692 *Nature* **562**, 367–372 (2018).
- 693 52. Quake, S. R., Consortium, T. S. & others. The *Tabula Sapiens*: A single cell transcriptomic atlas of  
694 multiple organs from individual human donors. *BioRxiv* (2021).
- 695 53. Tanay, A. & Seb e-Pedr os, A. Evolutionary cell type mapping with single-cell genomics. *Trends in*  
696 *Genetics* **37**, (2021).
- 697 54. Magnacca, K. N. & Price, D. K. New species of Hawaiian picture wing *Drosophila* (Diptera: Drosophil-  
698 idae), with a key to species. *Zootaxa* **3188**, 1–30 (2012).
- 699 55. Hardy, D. Review of the Hawaiian *Drosophila* (antopocerus) Hardy [insects]. *Proceedings Entomological*  
700 *Society of Washington* **79**, 82–95 (1977).
- 701 56. Hackman, W. On the genus *Scaptomyza* Hardy (Dipt., Drosophilidae) with descriptions of new species  
702 from various parts of the world. *Acta Zoologica Fennica* **97**, 1–73 (1959).
- 703 57. O’Grady, P., Kam, M., Val, F. do & Perreira, W. Revision of the *Drosophila mimica* subgroup, with  
704 descriptions of ten new species. *Annals of the Entomological Society of America* **96**, 12–38 (2003).
- 705 58. Hardy, D. *Diptera: Cyclorrhapha II, Series Schizophora Section Acalypterae I. Family Drosophilidae*.  
706 vol. 12 (University of Hawai’i Press, 1965).
- 707 59. O’Grady, P. M. *et al.* Phylogenetic and ecological relationships of the Hawaiian *Drosophila* inferred by  
708 mitochondrial DNA analysis. *Molecular Phylogenetics and Evolution* **58**, 244–256 (2011).
- 709 60. Lapoint, R. T., Magnacca, K. N. & O’Grady, P. M. Phylogenetics of the Antopocerus-Modified Tarsus  
710 clade of Hawaiian *Drosophila*: Diversification across the Hawaiian islands. *PLoS One* **9**, e113227 (2014).
- 711 61. Katoh, T., Izumitani, H. F., Yamashita, S. & Watada, M. Multiple origins of Hawaiian drosophilids:  
712 Phylogeography of *Scaptomyza hardy* (Diptera: Drosophilidae). *Entomological Science* **20**, 33–44 (2017).
- 713 62. Katoh, K. & Standley, D. M. MAFFT multiple sequence alignment software version 7: Improvements in  
714 performance and usability. *Molecular Biology and Evolution* **30**, 772–780 (2013).

- 715 63. Stamatakis, A. RAxML version 8: A tool for phylogenetic analysis and post-analysis of large phylogenies.  
716 *Bioinformatics* **30**, 1312–1313 (2014).
- 717 64. Li, B. & Dewey, C. N. RSEM: Accurate transcript quantification from RNA-seq data with or without a  
718 reference genome. *BMC Bioinformatics* **12**, 1–16 (2011).
- 719 65. Boussau, B. *et al.* Genome-scale coestimation of species and gene trees. *Genome Research* **23**, 323–330  
720 (2013).
- 721 66. Tung Ho, L. si & Ané, C. A linear-time algorithm for gaussian and non-gaussian trait evolution models.  
722 *Systematic Biology* **63**, 397–408 (2014).